Robust linear modelling in ElectroEncephaloGraphy can be obtained using single weights reflecting each single trials' dynamics

Cyril Pernet[1,2], Guillaume Rousselet[3], Ignacio Suay Mas[1], Ramon Martinez[4], Rand Wilcox[5] & Arnaud Delorme[4,6,7]

[1] Centre for Clinical Brain Sciences, University of Edinburgh, United Kingdom, [2] Neurobiology Research Unit, Copenhagen University Hospital, Rigshospitalet, Denmark, [3] Centre for Cognitive Neuroimaging, School of Psychology, University of Glasgow, United Kingdom, [4] Swartz Center for Computational Neurosciences, University of California San Diego, United States of America, [5] Department of Psychology, University of Southern California, United States of America, [6] Centre de Recherche Cerveau et Cognition, Université Toulouse III Paul Sabatier, Toulouse, France, [7] Centre National de la Recherche Scientifique, Centre de Recherche Cerveau et Cognition, Toulouse, France

Abstract

Being able to remove or weigh down the influence of outlier data is desirable for any statistical models. While Magnetic and ElectroEncephaloGraphic (MEEG) data used to average trials per condition, it is now becoming common practice to use information from all trials to build linear models. Individual trials can, however, have considerable weight and thus bias inferential results. Here, rather than looking for outliers independently at each data point, we apply the principal component projection (PCP) method at each channel, deriving a single weight per trial at each channel independently. Using both synthetic data and open EEG data, we show (1) that PCP is efficient at detecting a large variety of outlying trials; (2) how PCP derived weights can be implemented in the context of the general linear model with accurate control of type 1 family-wise error rate; and (3) that our PCP-based Weighted Least Square (WLS) approach leads to in increase in power at the group results comparable to a much slower Iterative Reweighted Least Squares (IRLS), although the weighting scheme is markedly different. Together, results show that WLS based on PCP weights derived upon whole trial profiles is an efficient method to weigh down the influence of outlier data in linear models.

Keywords: ElectroEncephaloGraphy, single trials, Weighted Least Squares, General Linear Model

Data availability: all data used are publicly available (CC0), all code (simulations and data analyzes) is also available online in the LIMO MEEG GitHub repository (MIT license).

Introduction

MEEG data are often epoched to form 3 or 4-dimensional matrices of, e.g., channel x time x trials and channel x frequency x time x trials. Several neuroimaging packages are dedicated to the analyses of such large multidimensional data, often using linear methods. For instance, in the LIMO MEEG toolbox (Pernet et al., 2011), each channel, frequency, and time frame is analyzed independently using the general linear model, an approach referred to as mass-univariate analysis. Ordinary Least Squares (OLS) are used to find model parameters that minimize the error between the model and the data. For least squares estimates to have good statistical properties, it is however expected that the error covariance off-diagonals are zeros, such that $Cov(e) = \sigma^2 I$, I being the identity matrix (Christensen, 2002) assuming observations are independent and identically distributed. It is well established that deviations from that assumption lead to substantial power reduction and to an increase in the false-positive rate. When OLS assumptions are violated, robust techniques offer reliable solutions to restore power and control the false positive rate. Weighted Least Squares (WLS) is one such robust method that uses different weights across trials, such that $Cov(e) = \sigma^2 V$, with V a diagonal matrix:

$$y = X\beta + e, \quad E(e) = 0, \quad Cov(e) = \sigma^2 V \qquad \textit{equation 1}$$

with y a n-dimensional vector (number of trials), X the n*p design matrix, β a p dimensional vector (number of predictors in X) and e the error vector of dimension n. The WLS estimators can then be obtained using an OLS on transformed data (eq. 2 and 3):

$$Wy = WX\beta + We, \quad E(e) = 0, \quad Cov(e) = \sigma^2 I \qquad \textit{equation 2}$$

$$\hat{\beta} = (X^T WX)^{-1} X^T Wy \qquad \textit{equation 3}$$

with W a 1*n vector of weights.

When applied to MEEG data, a standard mass-univariate WLS entails obtaining a weight for each trial but also each dimension analyzed, i.e. channels, frequencies and time frames. Following such procedure, a trial could be considered as an outlier or be assigned a low weight, for a single frequency or time frame, which is implausible given the well-known correlations of MEEG data over space, frequencies and time. We propose here that a single or a few consecutive data points should never be flagged as outliers or weighted down, and that a single weight per trial (and channel) should be derived instead, with weights taking into account the whole temporal or spectral profile. In the following, we demonstrate how the Principal Component Projection method (PCP - Filzmoser et al., 2008) can be used in this context, and how those weights can then be used in the context of the general linear model, applied here to event-related potentials.

Method

Trial-based Weighted Least Squares

An illustration of the method is shown in figure 1. Trial weights are computed as a distance among trials projected onto the main (>=99%) principal components space. Here, the principal components computed over the f time frames are those directions which maximize the variance across trials for uncorrelated (orthogonal) time periods (figure 1B). Outlier trials are points in the f-dimensional space which are far away from the bulk. By virtue of the PCA, these outlier trials become more visible along the principal component axes than in the original data space. Weights (figure 1E) for each trial are obtained using both the Euclidean norm (figure 1C, distance location) and the kurtosis weighted Euclidean norm (figure 1D, distance scatter) in this reduced PCA space (see Filzmoser et al., 2008 for details). We choose to exploit this simple technique because it is computationally fast given the rich dimensional space of EEG data and because it does not assume the data to originate from a particular distribution. The only constraint is that there are more trials present than time frames. For instance, with trials ranging from -50 ms to +650 ms, sampled at 250 Hz, the method requires at least 177 trials. The PCP algorithm is implemented in the *limo_pcout.m* function, distributed with the LIMO MEEG toolbox (https://limo-eeg-toolbox.github.io/limo_meeg/). The WLS solution, implemented in *limo_WLS.m*, consists of computing model beta estimates using weights from the PCP method on OLS standardized robust residuals, following three steps:

(1) After the OLS solution is computed, an adjustment is performed on residuals by multiplying them by $1/\sqrt{1-h}$ where h is a vector of Leverage points (i.e. the diagonal of the hat matrix $H = X(X'X)^{-1}X'$ where X is the design matrix). This adjustment is necessary because leverage points are the most influential on the regression space, i.e. they tend to have low residual values (Hoaglin & Welsch, 1978).
(2) Residuals are then standardized using a robust estimator of dispersion, the median absolute deviation to the median (MAD), and re-adjusted by the tuning function. Here we used the bisquare function. The result is a series of weights with high weights for data points having high residuals (with a correction for Leverage).
(3) The WLS solution is then computed following equation 3.

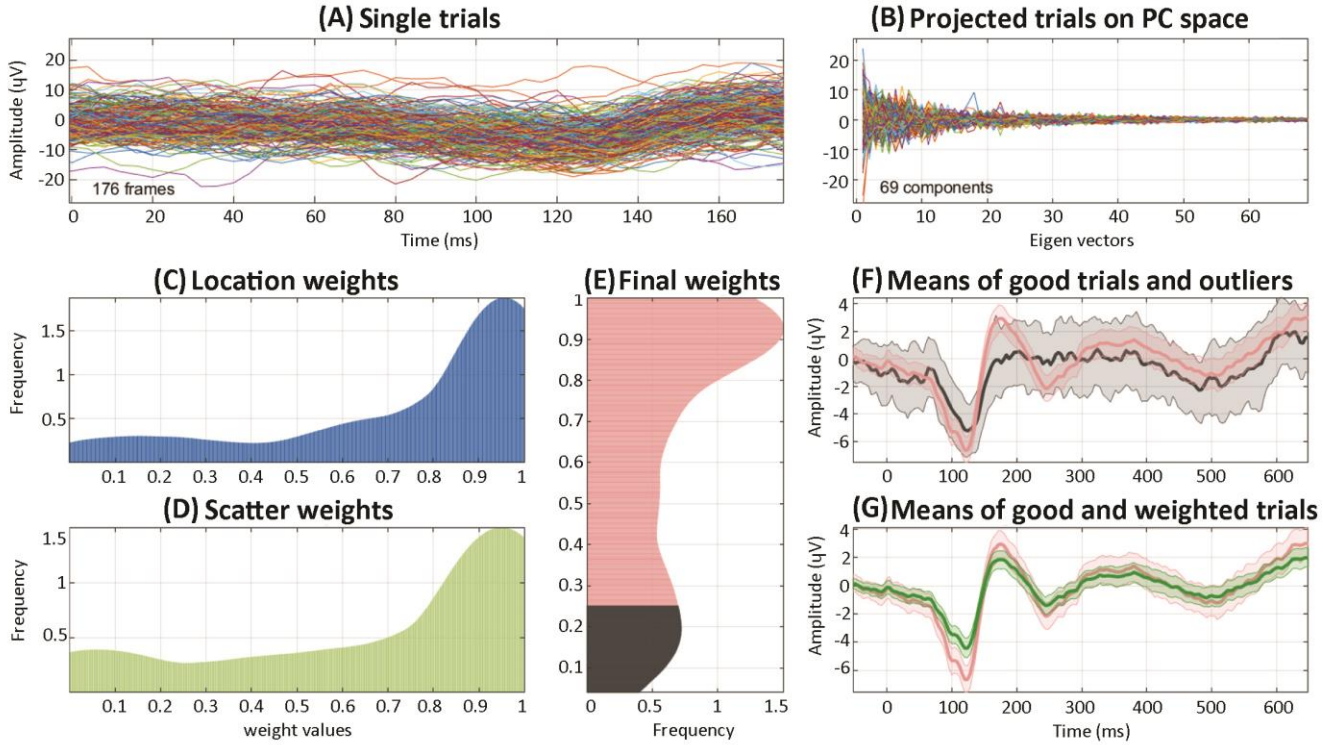

Figure 1. Illustration of the PCP weighting scheme using trials for 'famous faces' of the OpenNeuro.org publicly available ds002718 dataset in subject 3, channel 34 (see Section on empirical data analysis). Panel A shows the single-trial responses to all stimuli. The principal component analysis is computed over time, keeping the components explaining the most variance and summing to at least 99% of explained variance (giving here 69 eigenvectors i.e. 'independent time components' from the initial 176 time points) and the data are projected onto those axes (panel B). From the projected data onto the components, Euclidean distances for location and scatter are computed (panels C, D - showing smooth histograms of weights) and combined to obtain a distance for each trial. That distance is either used as weights in a linear model or used to determine outliers (panel E, with outliers identified for weights below ~0.27, shown in dark grey). At the bottom right, the mean ERP for trials classified as good (red) vs. outliers (black) and the weighted mean (green) are shown (panels F and G). Shaded areas indicate the 95% highest-density percentile bootstrap intervals.

Simulation-based analyses

A. *Outliers detection and parameters estimation.*

Simulated ERPs were generated to evaluate the classification accuracy of the PCP method and estimate the robustness to outliers and low signal-to-noise ratio of the WLS solution in comparison to an OLS solution and a standard Iterative Reweighted Least Squares (IRLS) solution which minimizes residuals at each time frame separately (implemented in *limo_IRLS.m*). To do so, we manipulated (i) the percentage of outliers (how robust is the method), testing for 10%, 20%, 30%, 40% or 50% of outliers; (ii) the signal to noise ratio (defined relative to the mean over time of the background activity); and (iii) the type of outliers. The first set of outliers were defined based on the added noise: white noise, pink noise, alpha oscillations and gamma oscillations. In these cases, the noise started with the P1 component and lasted ~ 200ms (see below). The second set of outliers were defined based on their amplitude, or outlier to signal ratio (0.5, 0.8, 1.2, and 1.5 times the 'true' N1 amplitude).

Synthetic data were generated for one channel, using the model developed by (Yeung et al., 2018). The simulated signal corresponded to an event-related potential with P1 and N1 components (100 ms long) added to background activity with the same power spectrum as human EEG, generating 200 trials of 500 ms duration with a 250 Hz sampling rate. Examples for each type of simulation are shown in figure 2 and results are based, for each case, on a thousand random repetitions. Performance of the PCP algorithm at detecting outlying synthetic EEG trials was investigated by computing the confusion matrix and mapping the true and false positives rates in the Receiver Operating space, and by computing the Matthew Correlation Coefficients (MCC). Robustness was examined by computing the Pearson correlations and the Kolmorov-Smirnov (KS) distances between the ground truth mean and the OLS, WLS, and IRLS means. Pearson values allowed to estimate the linear relationships between estimated means and the truth while KS distances provide a fuller picture of the overall differences in distributions. The code used to generate the ERP and the results are available at https://github.com/LIMO-EEG-Toolbox/limo_test_stats/tree/master/PCP_simulations.

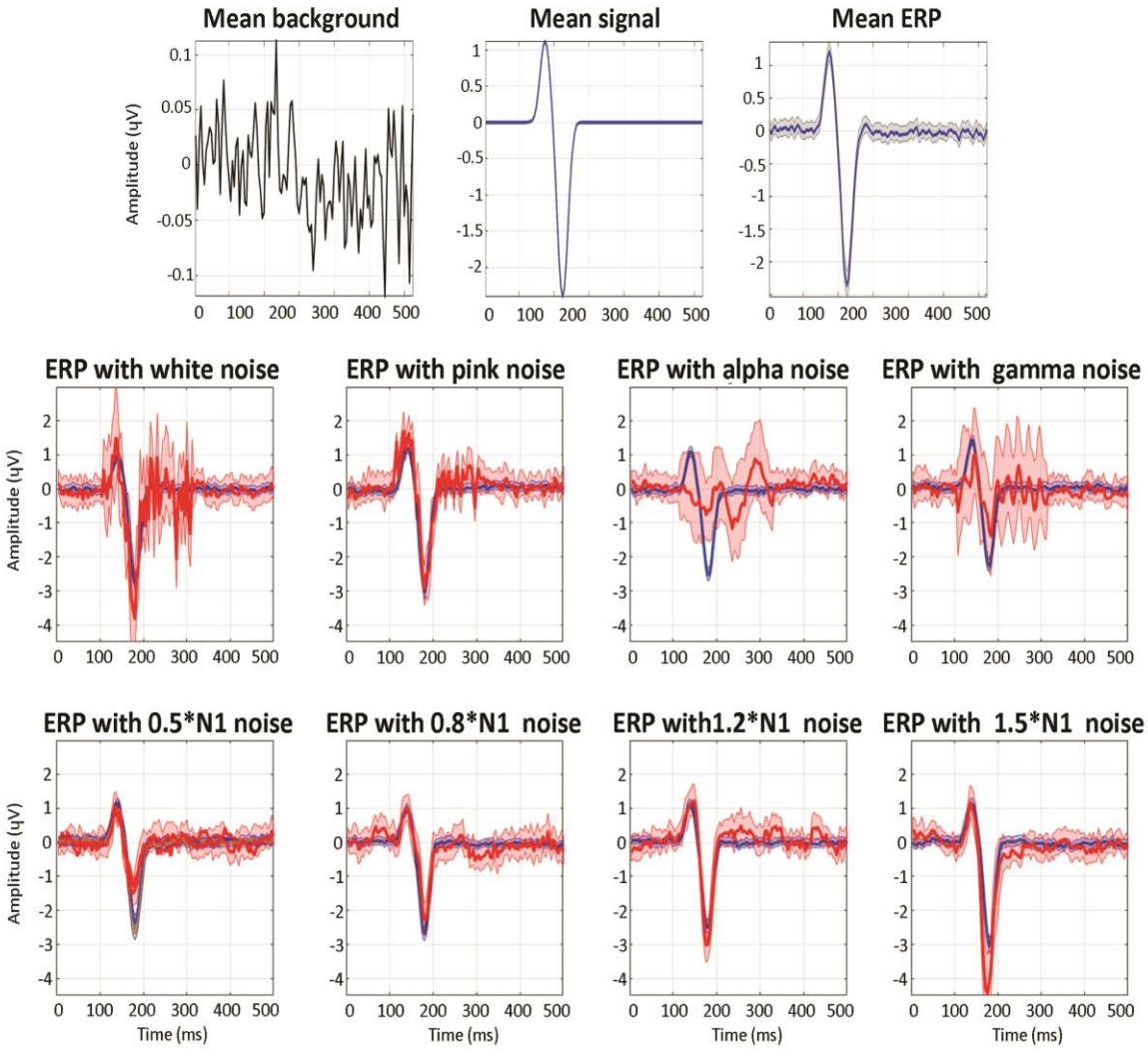

Figure 2. Illustration of simulated ERP ground truth with the different types of outlier trials. At the top is shown the mean background, mean signal and resulting generated ERP with it's 95% confidence intervals. In each subsequent subplot is shown the mean ERP ground truth from 160 trials with their 95% confidence intervals (blue) with a SNR of 1. The first row shows the mean ERP from outlier trials generated by adding white noise, pink noise, alpha or gamma oscillations; the second row shows the mean ERP from outlier trials generated with variable Outlier to Signal Ratio (OSR) on the N1 component.

B. Statistical inference.

Accurate estimation of model parameters (i.e. beta estimates in the GLM - equation 3) is particularly important because it impacts group-level results. Inference at the single-subject level may, however, also be performed and accurate p-values need, therefore, to be derived. Here, error degrees of freedom are obtained using the Satterwaithe approximation (equation 4).

$$dfe = tr([I - H]^T[I - H]) \quad \textit{equation 4}$$

with dfe the degree of freedom of the error, I the identity matrix and H the hat matrix

To validate p-values, simulations under the null were performed. Two types of data were generated: Gaussian data of size 120 trials x 100 time frames and EEG data of size 120 trials x 100 time frames with a P1 and N1 component as above, added to coloured background activity with the same power spectrum as human EEG. In each case, a regression (1 Gaussian random variable), an ANOVA (3 conditions of 40 trials - dummy coding) and an ANCOVA (3 conditions of 40 trials and 1 Gaussian random covariate) model were fitted to the data using the OLS, WLS and IRLS methods. The procedure was performed 10,000 times, leading to 1 million p-values per data/model/method combination and Type 1 errors with binomial confidence intervals were computed.

Empirical data analysis

A second set of analyses used the publicly available multimodal face dataset (Wakeman & Henson, 2016) to (i) investigate the PCP classification; (ii) validate the GLM implementation for type 1 error family-wise control at the subject level; (iii) evaluate group results, contrasting WLS against the OLS and IRLS methods. This analysis can be reproduced using the script @https://github.com/LIMO-EEG-Toolbox/limo_meeg/blob/master/resources/code/Method_validation.m

A. EEG Data and Preprocessing

The experiment consisted in the presentation of familiar, unfamiliar, and scrambled faces, repeated twice at various intervals, leading to a factorial 3 (type of faces) by 3 (repetition) design. The procedure followed (Pernet et al., 2021). EEG data were extracted from the MEG fif files, time corrected and electrode position re-oriented and saved according to EEG-BIDS (Pernet et al., 2019 - available at OpenNeuro 10.18112/openneuro.ds002718.v1.0.2.). Data were imported into EEGLAB (Delorme & Makeig, 2004) using *the bids-matlab-tools v5.2 plug-in* and non-EEG channel types were removed. Bad channels were next automatically removed and data filtered at 0.5Hz using *pop_clean_rawdata.m* of the *clean_radata* plugin v2.2 (transition band [0.25 0.75], bad channel defined as a flat line of at least 5sec and with a correlation to their robust estimate based on other channels below 0.8). Data were then re-referenced to the average (*pop_reref.m*) and submitted to an independent component analysis (Onton et al., 2006) (*pop_runica.m* using the runnica algorithm sphering data by the number of channels -1). Each component was automatically labelled using the *ICLabel* v1.2.6 plug-in (Pion-Tonachini et al., 2019), rejecting components labeled as eye movements and muscle activity above 80% probability. Epochs were further cleaned if their power deviated too much from the rest of the data using the Artifact Subspace Reconstruction algorithm (Kothe & Makeig, 2013) (*pop_clean_rawdata.m*, burst criterion set to 20).

B. High vs. low weight trials and parameters estimation.

At the subject level, ERP were modelled at each channel and time frame with the 9 conditions (type of faces x repetition) and beta parameter estimates obtained using OLS, WLS, and IRLS. For each subject, high vs. low weight trials were compared with each other at the channel showing

the highest between trials variance to investigate what ERP features drove the weighting schemes. High and low trials were defined a priori as trials with weights (or mean weights for IRLS) below the first decile or above the 9th decile. We used two samples bootstrap-t on 20% trimmed means to compare these quantities in high and low trials in every participant: temporal SNR (the standard deviation over time); global power (mean of squared absolute values, Parseval's theorem); autocorrelation (distance between the 2 first peaks of the power spectrum density, Wiener-Khinchin theorem). A similar analysis was conducted at the group level averaging across trials metrics. Computations of these three quantities have been automatized for LIMO MEEG v3.0 in the *limo_trialmetric.m* function.

C. Statistical inference.

In mass-univariate analyses, once p-values are obtained, the family-wise type 1 error rate can be controlled using the distribution of maxima statistics from data generated under the null hypothesis (Pernet et al., 2015). Here, null distributions were obtained by first centering data per conditions, i.e. the mean is subtracted from the trials in each condition, such that these distributions had a mean of zero, but the shape of the distributions is unaffected. We then bootstrap these centred distributions (by sampling with the replacement), keeping constant the weights (since they are variance stabilizers) and the design. We computed 2,500 bootstrap estimates per subject. A thousand of these bootstrap estimates were used to compute the family-wise type 1 error rate (FWER), while maxima and cluster maxima distributions were estimated using the from 500 to 1,500 bootstraps estimates from the remaining set (e.g. use 500 estimates to build the null distribution of maxima, and test FWER using 1000 draws, redo the analysis with 600 estimates to build the null distribution of maxima, and test FWER using again the 1000 independent draws, etc). This allowed analysing the convergence rate, i.e. how many resamples are needed to control the FWER. Since OLS was already validated in Pernet et al. (2015), here we present WLS results. Statistical validations presented here and other statistical tests implemented in the LIMO MEG toolbox v3.0 (GLM validation, robust tests, etc.) are all available at https://github.com/LIMO-EEG-Toolbox/limo_test_stats/wiki.

D. Performance evaluation at the group level.

At the group level, we computed 3 by 3 repeated measures ANOVA (Hotelling $T^{\wedge 2}$ tests) separately on OLS, WLS, and IRLS estimates, with the type of faces and repetition as factors. Results are reported using both a correction for multiple comparisons with cluster-mass and with TFCE (threshold-free cluster enhancement) at $p<.05$ (Maris, E. & Oostenveld, R., 2007; C.R. Pernet et al., 2015).

In addition to these thresholded maps, distributions were compared to further understand where differences originated from. First, we compared raw effect sizes (Hotelling T^2) median differences between WLS vs. OLS and WLS vs. IRLS for each effect (face, repetition and interaction), using a percentile t-test with alphav adjusted across all 6 tests using the Hochberg step-up procedure. This allowed checking if differences in results were due to effect size differences. Then, since multiple comparison correction methods are driven by the data

structure, we compared the shapes of the F value and of the TFCE value distributions (tfce reflecting clustering). Each distribution was standardized (equation 5) and WLS vs. OLS and WLS vs. IRLS distributions compared using shift function analyses (Rousselet et al., 2017).

$$Yzi = \frac{(Yi - median(Y)}{\sqrt{(pi/2)} * MAD(Y)} \quad \textit{equation 5}$$

with Yzi the standardized data, Y the data, and MAD the median absolute deviation

Results

Outliers detection

While the PCP method is used in the GLM to obtain weights and not to remove outliers directly, simulations allowed to better understand what kind of trials are weighted down and how good the method is at detecting such trials. Figure 3 shows all the results for ERP simulated with a SNR of 1. Similar results were observed when using a SNR of 2 (supplementary figure 1). First and foremost, in all cases and for up to 40% of outlying trials, the PCP data are located in the upper left corner of the ROC space, indicating good performances. When reaching 50% of outliers, the true positive rate falls down to ~40% and the false positive rate remains below 40%. This is best appreciated by looking at the plots showing perfect control over false positives when data are contaminated with up to 40% of white, alpha, and gamma outliers. For those cases, the Matthew Correlation Coefficients also remain high (>0.6) although not perfect (not =1), indicating some false negatives. Compared with other types of noise, pink noise elicited very different results, with Matthew Correlation Coefficients around 0 indicating chance classification level. Results from amplitude outliers also show Matthew Correlation Coefficients close to 0 with a linear increase in false positives and linear decrease in false positives as the percentage of outliers increases, i.e., the PCP method did not detect amplitude changes around peaks. These results are simply explained by the principal components being computed over time frames, and outliers with pink noise and weaker or stronger N1 do not show different 'directions' (eigen vectors) in this dimension when decomposing the covariance matrix, i.e. their temporal profiles do not differ from the ground truth.

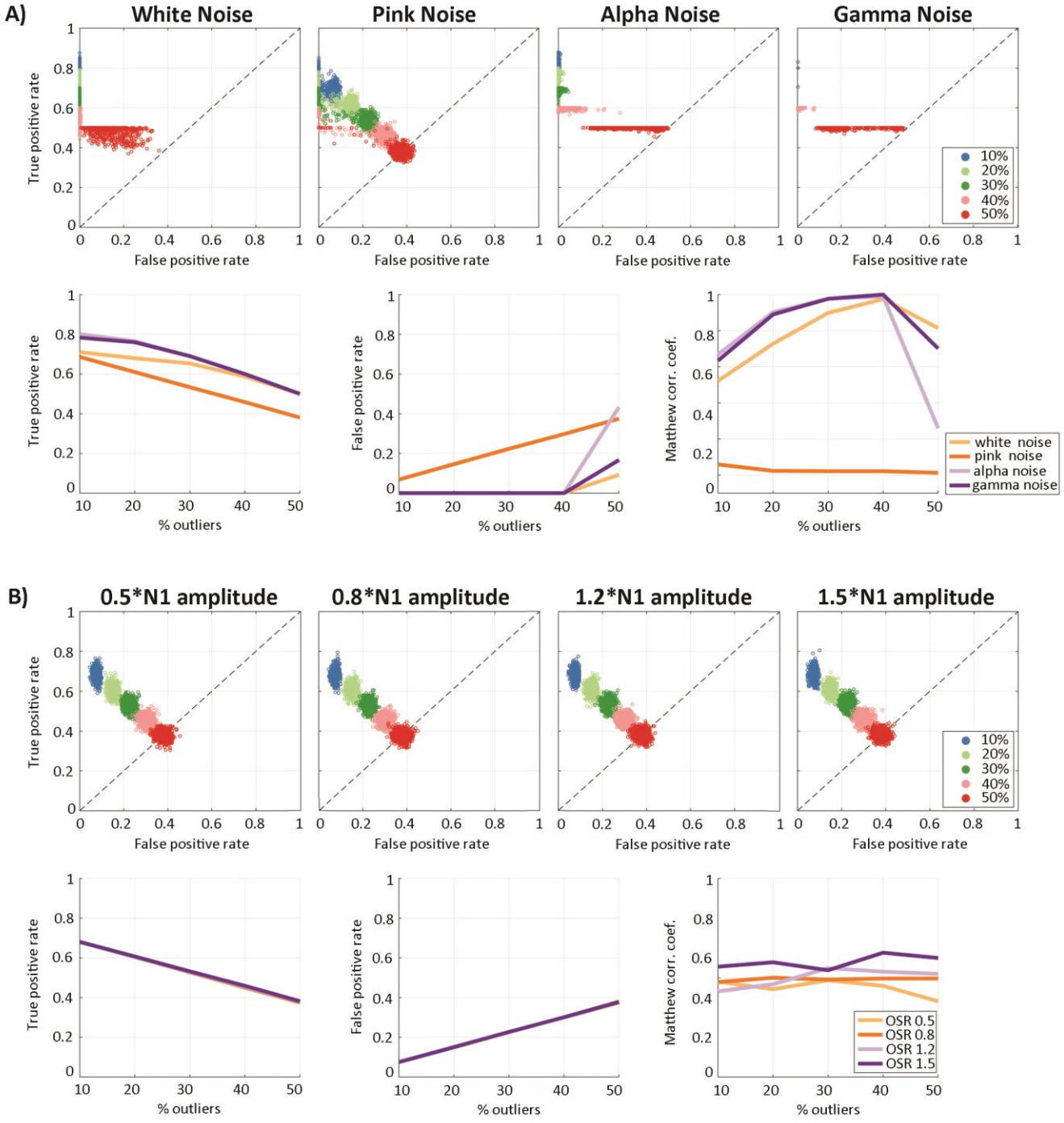

Figure 3. PCP performance at detecting outlying trials with a SNR of 1. (A) Results for outliers affected by white noise, pink noise, alpha, and gamma oscillations. (B) Results for trials affected by amplitude changes over the N1 component (0.5, 0.8, 1.2, 1.5 times the N1). The scatter plots map the Receiver Operating Characteristic Space (False Positive rate vs. True Positive rate); the curves display, from left to right, the median True Positive rate, False Positive rate, and Matthew Correlation Coefficients.

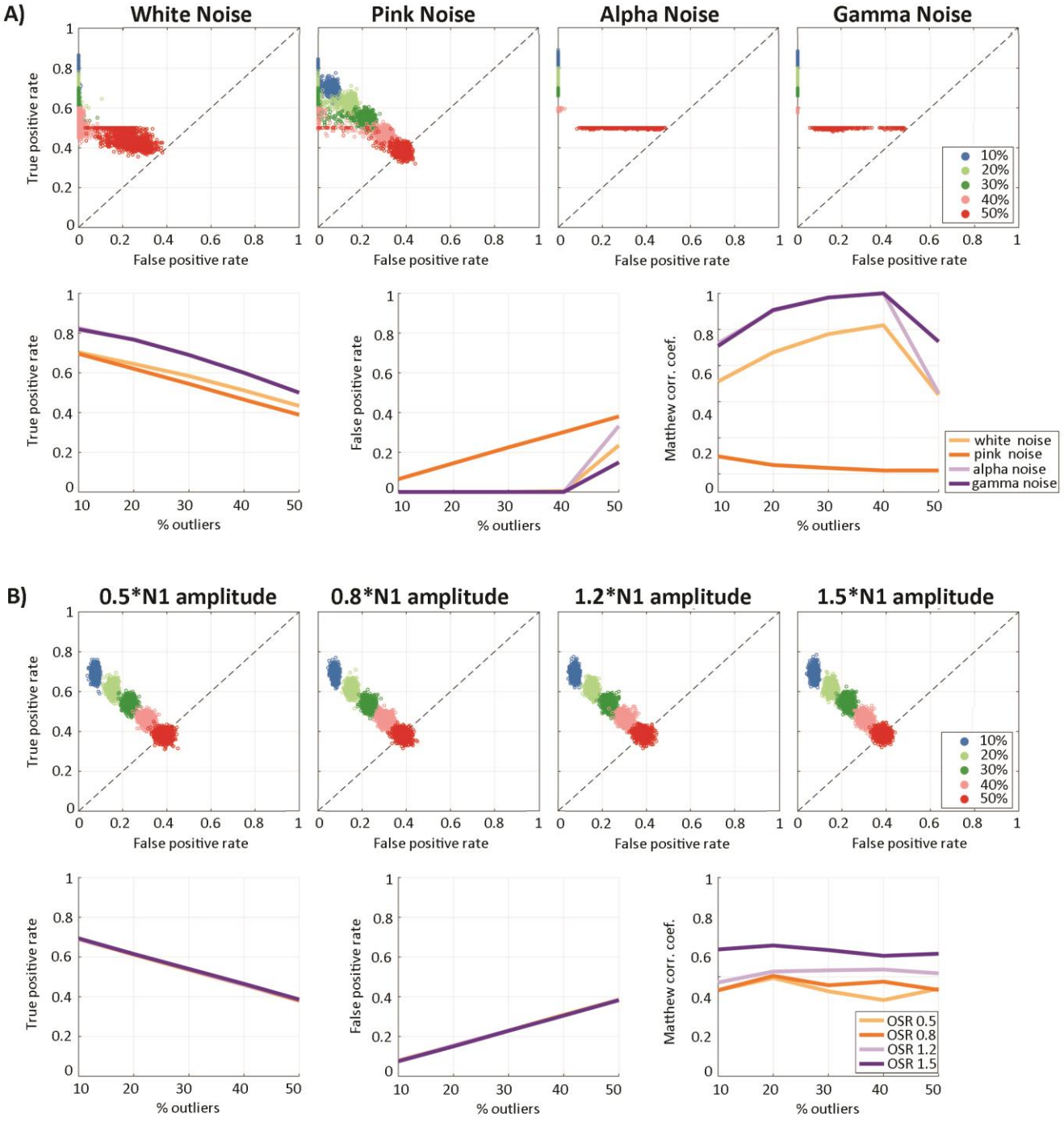

Supplementary Figure 1. PCP performance at detecting outlying trials with a SNR of 2. (A) Results for outliers affected by white noise, pink noise, alpha, and gamma oscillations. (B) Results for trials affected by amplitude changes over the N1 component (0.5, 0.8, 1.2, 1.5 times the N1). The scatter plots map the Receiver Operating Characteristic Space (False Positive rate vs. True Positive rate); the curves display, from left to right, the median True Positive rate, False Positive rate, and Matthew Correlation Coefficients.

306 *High vs. low trial weights*
307
308 The classification for real ERP data confirmed results observed with simulations: the PCP
309 algorithm weighted down trials with different dynamics from the bulk. Single subject analyses
310 (supplementary table 1) and group analyses (figure 4) for WLS showed that trials with a low
311 weight are less smooth than trials with a high weight (higher temporal variance ~10 vs. 7.26uV
312 and power ~131 vs. 69dB, lower autocorrelation 11 vs. 12.25ms), despite having similar spectra
313 (as expected from data filtering and artefact reduction). In comparison, trials with low and high
314 mean weight based on IRLS, were similar on those metrics (temporal variance ~9 vs. 7uV, and
315 power ~126 vs. 65dB, autocorrelation 12.25 vs. 12ms). While 11 out of 18 subjects show
316 maximum between-trial variance on the same channels for WLS and IRLS, only 28% of low weight
317 trials were the same vs. 56% of high weight trial, further indicating that the weighting scheme
318 from WLS does not reflect amplitude variations only, as does IRLS.
319
320

	tSNR difference (uV)		*Power difference (dB)*		*autocorrelation difference (ms)*	
	WLS	*IRLS*	*WLS*	*IRLS*	*WLS*	*IRLS*
s2	*[-0.03 0.54]*	*[0.26 1.14]*	*[-2 6]*	*[3 18]*	*[-8.5 1.8]*	*[5.09 16.4]*
s3	*[2.35 2.92]*	*[-4.48 -2.34]*	*[35 50]*	*[-55 -22]*	*[-3.9 3.5]*	*[16.6 45.9]*
s4	*[0.14 069]*	*[1.9 3.43]*	*[1 13]*	*[39 64]*	*[-13 -6.7]*	*[-12.8 3.2]*
s5	*[4.03 8.25]*	*[10.7 13.57]*	*[77 200]*	*[297 382]*	*[-13 -4.7]*	*[-14.6 -4.9]*
s6	*[1.51 2.87]*	*[-0.74 1.98]*	*[24 48]*	*[-6 33]*	*[-4.8 -0.39]*	*[-0.6 17.8]*
s7	*[1.16 5.1]*	*[2.44 5.26]*	*[38 141]*	*[54 129]*	*[-4 11.1]*	*[-7.3 11.2]*
s8	*[7.49 8.21]*	*[7.57 8.55]*	*[154 173]*	*[159 183]*	*[-24 -19.8]*	*[-20.2 -14.1]*
s9	*[2.97 7.96]*	*[-4.55 0.44]*	*[52 169]*	*[-74 28]*	*[-16 -7.1]*	*[-1.5 7.1]*
s10	*[-0.61 0.9]*	*[-3.47 2.27]*	*[-11 11]*	*[-107 102]*	*[0.9 9.1]*	*[-0.2 1.5]*
s11	*[-0.73 4.46]*	*[4.57 7.27]*	*[-11 168]*	*[123 200]*	*[-2.9 1.4]*	*[0 7.8]*
s12	*[6.69 11.17]*	*[-2.06 4.85]*	*[149 250]*	*[-98 93]*	*[-31 -22]*	*[-13.1 -2.7]*
s13	*[-5.06 0.1]*	*[-6.8 2.91]*	*[-222 2]*	*[-285 142]*	*[4.4 12]*	*[-6.2 0.19]*
s14	*[4.81 7.63]*	*[3.54 7.77]*	*[174 270]*	*[123 270]*	*[-0.4 24]*	*[-6.9 13.3]*
s15	*[1.69 3.91]*	*[-0.97 2.06]*	*[36 93]*	*[-20 51]*	*[-6.5 1.1]*	*[1.8 10.5]*
s16	*[-6.85 8.4]*	*[-2.13 13.82]*	*[-164 300]*	*[-65 444]*	*[-8.3 8.7]*	*[-16 14.1]*
s17	*[2.34 3.72]*	*[2.31 4.09]*	*[34 68]*	*[45 83]*	*[-29.4 -15.9]*	*[-13.8 2.4]*

s18	*[0.54 1.28]*	*[-0.64 1.86]*	*[6 20]*	*[-3 27]*	*[-15.7 -2.43]*	*[-28.8 11.4]*
s19	*[-0.39 0.71]*	*[-0.40 0.57]*	*[-8 16]*	*[-9 17]*	*[-6.9 -1.3]*	*[-7.1 -1.5]*

Supplementary Table 1. Subjects 95% percentile bootstrap confidence intervals of differences between high and low trials trimmed means obtained using PCP-WLS or IRLS at channels with the highest between trials variance. Intervals which do not include 0 (i.e., the difference between high vs. low trials is statistically significant) are shown on gray background.

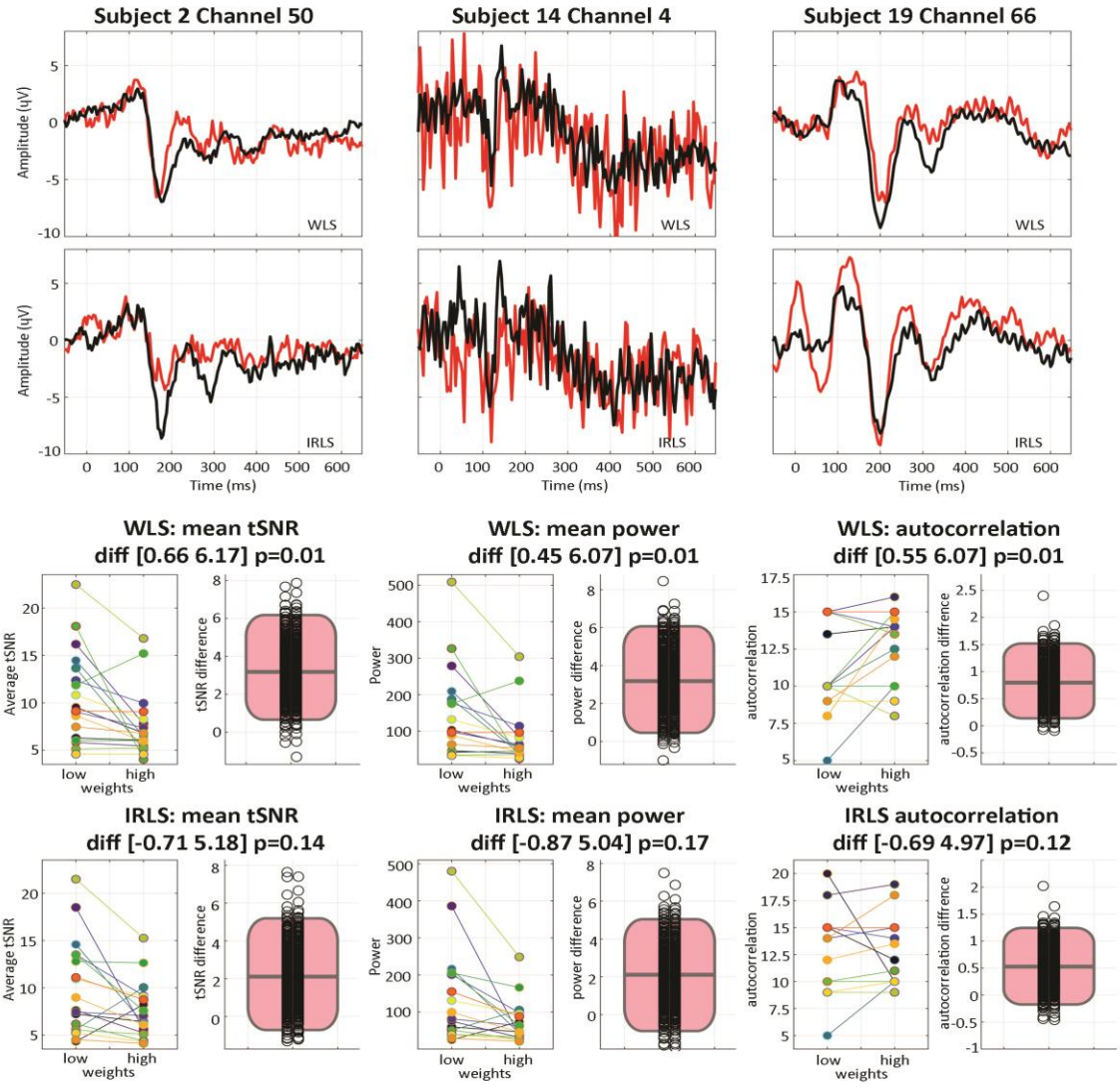

Figure 4. Face ERPs computed using low and high weight trials. The top of the figure displays the mean of low weight (red) and high weight (black) trials over right posterior temporal (subject 2, channel 50), left frontal (subject 14 channel 4), and left posterior central (subject 19, channel 66) areas obtained either with the PCP-WLS or the IRLS methods - as illustration of differences in tSNR, power, and autocorrelation. The bottom of the figure displays single subject mean tSNR, power and autocorrelation (scatter plots) along with the percentile bootstrap difference between low and high weight trials (black circles data points are the bootstrap trimmed mean differences and the pink rectangles show the 20% trimmed mean and 95% confidence intervals).

335 *Estimation and Robustness*
336
337 The effect of adding outliers on the mean can be seen in figure 5 and supplementary figure 2.
338 The standard mean, i.e. the ordinary least squares ERPs, shows an almost linear decrease in
339 Pearson correlations and linear increase in KS distances to the ground truth as the percentage of
340 outlier increases, an expected behaviour since OLS are not robust. Our reference robust
341 approach, IRLS, shows robustness to white noise, alpha, and gamma oscillations with higher
342 Pearson correlations than the OLS. Yet it performed worse than the OLS with pink noise and
343 amplitude outliers showing lower correlations with the ground truth, despite having similar KS
344 distances for all cases. As the IRLS solution for pink noise and amplitude outliers weights data to
345 minimize residuals at each time point separately, these are also expected results, resulting in an
346 average distance (over time) larger than OLS. The new WLS approach showed stronger resistance
347 to outliers for white noise, alpha and gamma oscillations than the IRLS approach, with higher
348 Pearson correlations. For pink noise and N1 amplitude outliers, it performs as the IRLS, despite
349 different KS distances. The IRLS algorithm attenuates the influence of those data points that differ
350 from the ground truth, but this may be from different trials at different time points. By doing so,
351 KS distances to the ground truth were similar or lower (for alpha and gamma oscillations) than
352 the OLS. The WLS approach attenuates the influence of trials with different time courses and
353 thus, the WLS ERP mean is affected at every time point, even if the detection concerns a small
354 part of the time course, leading to higher KS distances even with a small number of outliers.
355 Conversely, the WLS ERP gets closer to the ground truth when the number of outliers is high
356 (white noise, apha, gamma oscillations up to 40%) or stay constant independently of the number
357 of outliers (pink noise, N1 amplitude outliers).

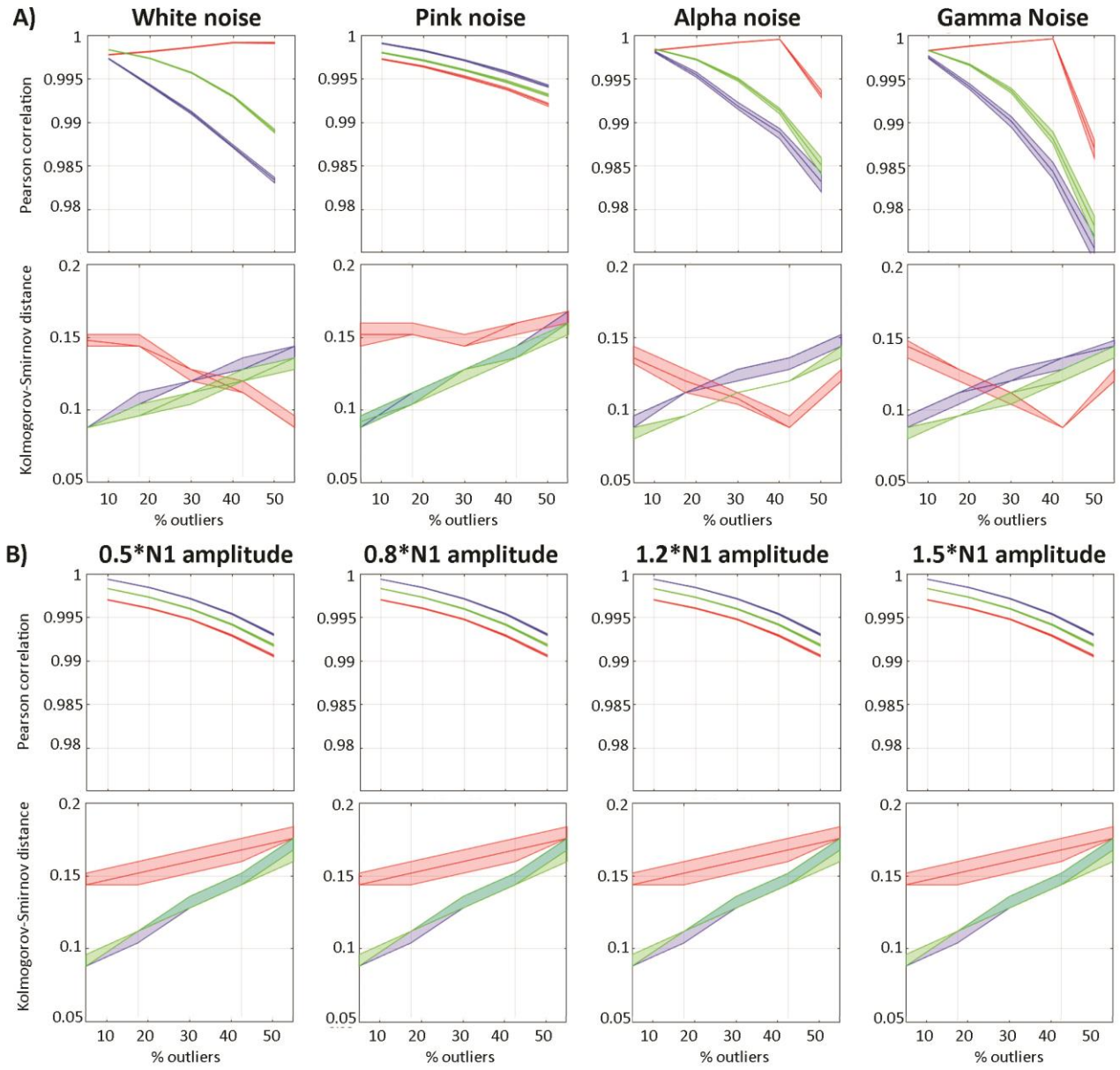

Figure 5. Robustness of the PCP method to outlying trials with a SNR of 1. The upper part of the figure shows median and 95% CI results for outliers affected by white noise, pink noise, alpha and gamma oscillations and the bottom part shows results for trials affected by amplitude changes over the N1 component (0.5, 0.8, 1.2, 1.5 times the N1). Mean Pearson correlations indicate how similar the reconstructed means (OLS in blue, IRLS in green, WLS in red) are to the ground truth, while mean Kolmogorov-Smitnov distances indicate how much the overall distribution of values differ from the ground truth.

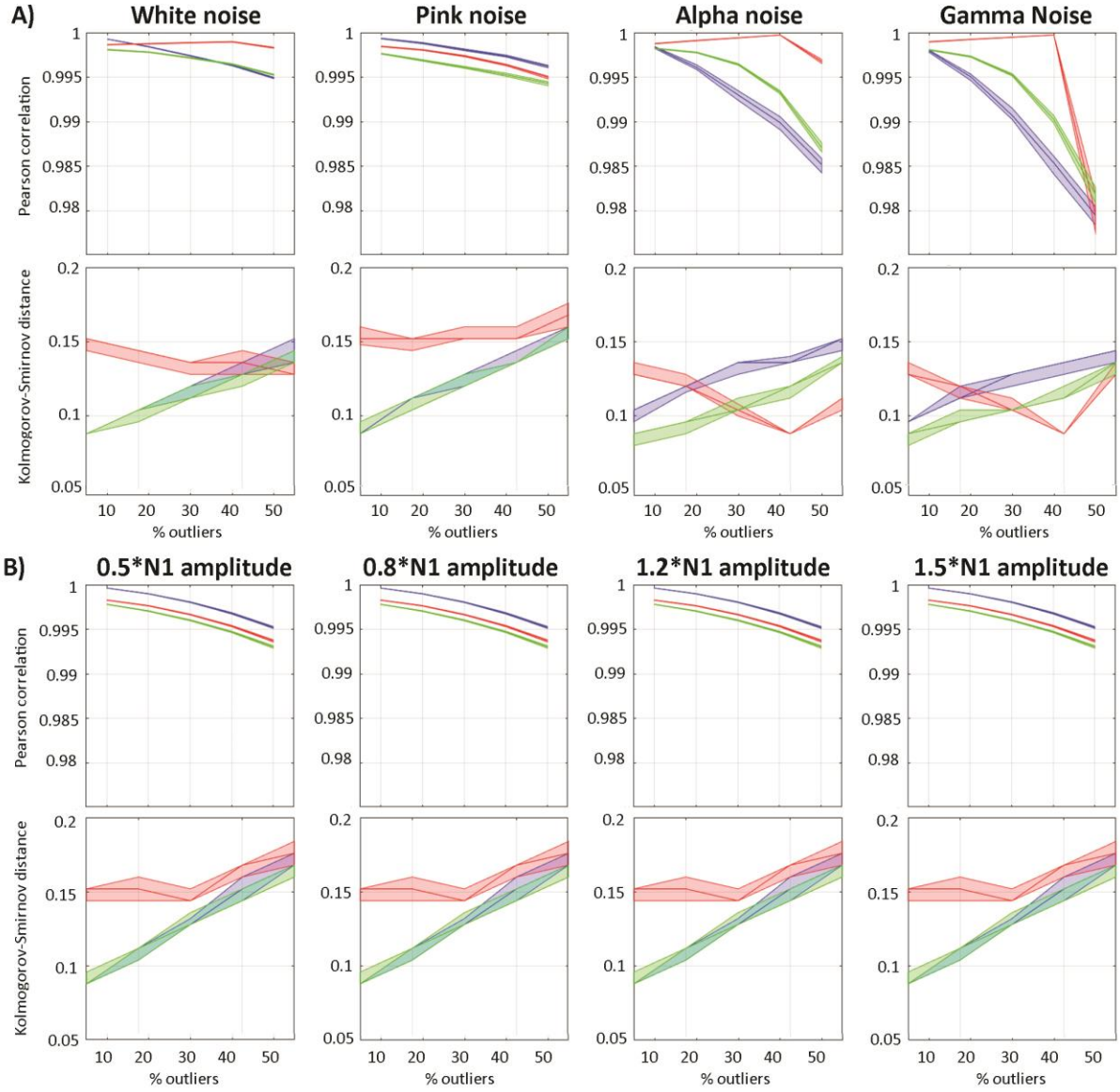

Supplementary figure 2. Robustness of the PCP method to outlying trials with a SNR of 2. The upper part of the figure shows median and 95% CI results for outliers affected by white noise, pink noise, alpha and gamma oscillations and the bottom part shows results for trials affected by amplitude changes over the N1 component (0.5, 0.8, 1.2, 1.5 times the N1). Mean Pearson correlations indicate how similar the reconstructed means (OLS in blue, IRLS in green, WLS in red) are to the ground truth, while mean Kolmogorov-Smitnov distances indicate how much the overall distribution of values differ from the ground truth.

Statistical inference for single subjects

The average type 1 error rate for every channel and time frame tested with simulated data is at the nominal level (5%) for OLS. Results also show that IRLS are a little lenient, with small but significantly smaller p-values than expected, leading to an error rate of ~0.055. Conversely, WLS

are conservative for simulated ERP, with p-values slightly too high, giving a type 1 error rate of ~0.04) and lenient with purely Gaussian data (type 1 error ~0.065 – table 1). This behaviour of WLS is caused by the PCP method which optimizes weights based on distances across time, except that with simulated Gaussian data there is no autocorrelation and the PCA returns a much higher number of dimensions, leading to a meaningless feature reduction and thus meaningless trial distances and weights.

		Null Gaussian	Null ERP
Regression	OLS	[0.0495 0.0503]	[0.0498 0.0507]
	WLS	[0.0636 0.0645]	[0.0400 0.0408]
	IRLS	[0.0555 0.0564]	[0.0527 0.0536]
ANOVA	OLS	[0.0493 0.0502]	[0.0493 0.0501]
	WLS	[0.0695 0.0706]	[0.0374 0.0382]
	IRLS	[0.0575 0.0584]	[0.0540 0.0549]
ANCOVA condition	OLS	[0.0494 0.0502]	[0.0493 0.0502]
	WLS	[0.0699 0.0709]	[0.0379 0.0386]
	IRLS	[0.0578 0.0587]	[0.0546 0.0555]
ANCOVA covariate	OLS	[0.0496 0.0505]	[0.0496 0.0504]
	WLS	[0.0638 0.0648]	[0.0410 0.0418]
	IRLS	[0.0563 0.0572]	[0.0538 0.0547]

Table 1. Type I error rate binomial 95% confidence intervals at every time frames and channels for simulated data under the null hypothesis.

The WLS family-wise type 1 error rate (i.e. controlling the error for statistical testing across the whole data space) examined using nullified ERP data from Wakeman and Henson (2015) shows a good probability coverage for both maximum and cluster statistics with 95% confidence intervals overlapping with the expected nominal value (figure 6). Individual mean values ranged from 0.039 to 0.070 for maximum statistics (across subject average 0.052) and 0.044 to 0.07 for spatial-temporal clustering (across subject average 0.051). Those results do not differ significantly from OLS results (paired bootstrap t-test). Additional analyses based on the number of of bootstraps used to build the null distribution indicate that 800 to a 1000 bootstraps are enough to obtain stable results, and that the errors do not appear at any spatial-temporal locations, i.e. there are no sampling bias (maximum number of error occurring at the same location was 0.05% using maximum statistics and 0.9% using spatial-temporal clustering, see bottom for figure 6, error density maps).

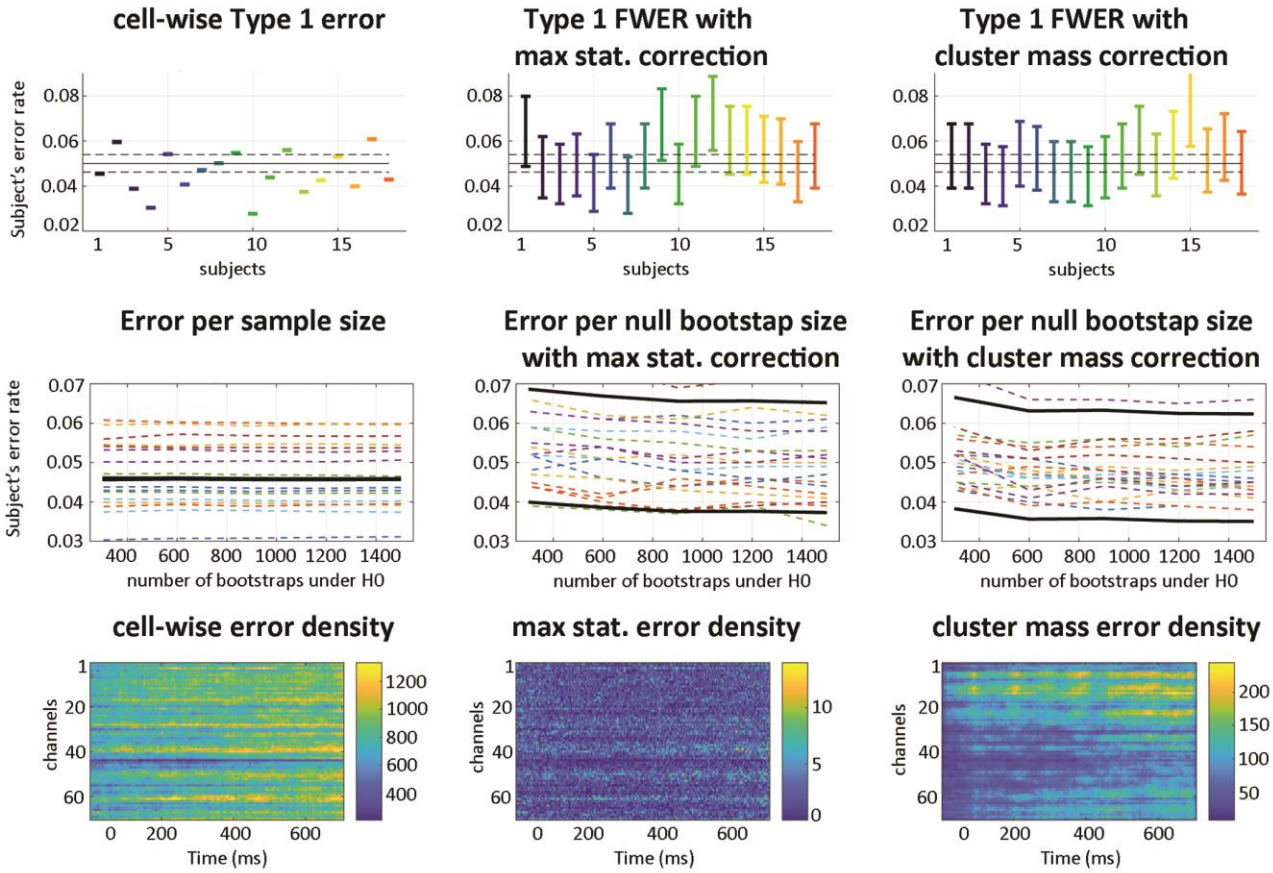

Figure 6. Type 1 error rates under the null using the PCP-WLS method. On the top row are shown the subjects' error rates: cell-wise, i.e. averaged across all time frames and channels, and corrected for the whole data space, i.e. type 1 family wise error rate using either the distribution of maxima or the distribution of the biggest cluster-masses. Results are within the expected range (marked by dotted black lines) with overlapping 95% confidence intervals for maximum statistics and spatial-temporal clustering. On the middle row are shown the effect of the number of resamples, with the tick lines representing the 95% average confidence interval. The cell-wise error is not affected since it does not depend directly on this parameter to estimate the null (left) while using maximum statistics and cluster-mass distribution estimates show a stronger dependency with results stable after 800 to 1000 bootstraps. On the bottom row are shown error density maps (sum of errors out of 27000 null maps). The cell-wise error (i.e. no correction for multiple comparisons) shows that errors accumulate, with some channels showing many consecutive time frames with 5% error. By contrast, maximum statistics (middle) and the maximum cluster-masses (right) do not show this effect (maxima at 0.05% and 0.9%), suggesting little to no spatial bias in sampling.

Performance evaluation at the group level

Repeated measures ANOVAs using parameter estimates from each method revealed 2 spatial-temporal clusters for the face effect for both WLS and IRLS, but only the 1st cluster was declared significant using OLS (table 2). The expected results (Wakeman & Henson, 2015) with full faces having stronger N170 responses than scrambled faces are replicated for all approaches.

Maximum differences were observed over the N170 only when using OLS parameters. Using WLS and IRLS gave maxima much later (P280), a result also observed when using TFCE rather than spatial-temporal clustering. In each case, a repetition effect was also observed in a much more consistent way among methods with the second presentation of stimuli differing from the 1st and 3rd presentations (figure 7).

	OLS	WLS	IRLS
Face effect			
cluster 1	140ms to 504ms, max=74, p=0.002 at 184ms channel EEG049	140ms to 424ms, max=64, p= 0.002 at 280ms channel EEG017	136ms to 432ms, max=74, p= 0.002 at 292ms channel EEG006
cluster 2		440ms to 648ms, max=17.6, p= 0.032 at 616ms channel EEG057	520ms to 648ms, max=22, p= 0.032 at 636ms channel EEG055
TFCE	max=74, p=0.026 at 184ms channel EEG049	max=64, p=0.012 at 280ms channel EEG017	max=74, p=0.012 at 292ms channel EEG006
Repetition effect			
cluster 1	232ms to 648ms, max=50, p= 0.001 at 588ms channel EEG057	232ms to 648ms, max=51, p= 0.001 at 612ms channel EEG045	236ms to 648ms, max=52, p= 0.001 at 588ms channel EEG057
TFCE	max=50, p=0.002 at 588ms channel EEG057	max=51, p= 0.001 at 612ms channel EEG045	max=52, p= 0.001 at 588ms channel EEG057

Table 2: Face and repetition effects results using cluster-mass correction and TFCE for each of the three methods.

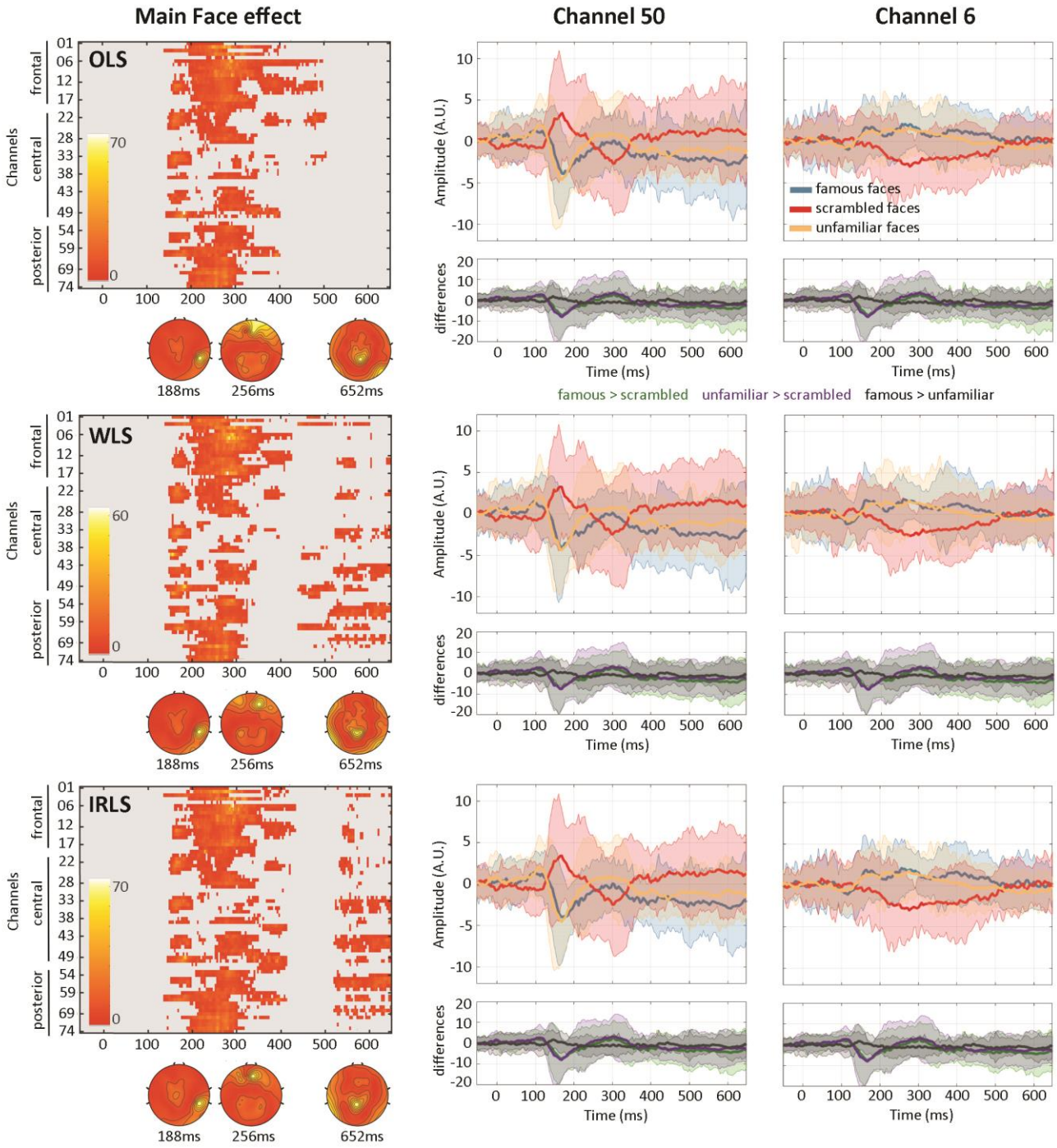

*Figure 7. Face group effects observed using OLS, WLS or IRLS 1st level derived parameters. On the left hand side is shown the full channels * times thresholded maps using cluster-mass (p<.05) with topographies over maxima. In the middle and right hand side are shown time courses of the mean parameter estimates per condition (blue, red, orange) and condition differences (green, purple, black) over channel 50 (right inferior-temporal) and channel 6 (middle anterior frontal).*

From the statistical maps, it can readily be observed that group results using 1st level WLS parameter estimates lead to smaller F values. Median differences in Hotelling T^2 values show that effects were always smaller compared to using parameter estimates from OLS or IRLS (Supplementary tables 2, 3 & table 3). Considering uncorrected p-values, this translates into less statistical power (Face effect OLS 34% WLS 31% IRLS 34% of significant data frames, Repetition effect OLS 39% WLS 35% IRLS 39% of significant data frames). Results based on corrected p-value based on clustering showed however more statistical power for the Face effect (OLS 20% WLS 22% IRLS 25% of significant data frames with cluster mass and 3%, 5% 3% of significant data frames with TFCE), and mixed results for the Repetition effect (OLS 31% WLS 28% IRLS 31% of significant data frames with cluster mass and 7%, 8% 7% of significant data frames with TFCE).

Comparison of standardized distributions for the face effect and repetition effect showed a general trend for more right skewed F-value and TFCE-value for WLS distributions than for OLS and IRLS distributions vs. shorter tail for the interaction effect (figure 8). For the face effect, WLS did not differ significantly from OLS or from IRLS when testing F-value deciles while TFCE values differed significantly, from the 2nd decile onward when compared to OLS, and for deciles 2,3,4,7,8,9 compared to IRLS. For the repetition effect, WLS differed from OLS on deciles 2,7,8,9 for both F-values and TFCE values while it differed from IRLS on decile 9 only when looking at F-values, and deciles 2,5,8,9 when looking at TFCE values. Finally, for the interaction effect, WLS did not differ from OLS or IRLS in terms of F-values but had significantly weaker TFCE values than OLS (deciles 1,3,6,7,8,9) and IRLS (all deciles but the 4th).

	face effect	repetition effect	interaction effect
WLS vs OLS	-0.32 [-0.36 -0.28]	-0.54 [-0.59 -0.48]	-0.21 [-0.29 -0.13]
WLS vs IRLS	-0.34 [-0.39 -0.30]	-0.53 [-0.58 -0.48]	-0.14 -0.21 -0.08]

Table 3. Median differences in Hotteling T^2 values for each effect tested with percentile bootstrap 95% confidence intervals (p=0.001).

		OLS	WLS	IRLS
Cluster 1 Channel 50	Famous Faces vs. Scrambled	-4.93 [-12.2 2.32]	-4.52 [-11.39 2.34]	-5.82 [-12.76 1.11]
	Unfamiliar Faces vs. Scrambled	-4.77 [-12.42 2.86]	-4.64 [-13.02 3.72]	-5.19 [-11.93 1.54]
	Famous vs Unfamiliar Faces	-0.15 [-3.13 2.81]	0.12 [-3.28 3.53]	-0.62 [-4.86 3.60]

Cluster 1 Channel 6	Famous Faces vs. Scrambled	2 [-5.25 9.25]	1.71 [-5.16 8.59]	1.68 [-6.05 9.41]
	Unfamiliar Famous Faces vs. Scrambled	3.21 [-5.80 12.22]	2.20 [-5.97 10.38]	2.95 [-6.08 11.99]
	Famous vs Unfamiliar Faces	-1.20 [-5.72 3.30]	-0.49 [-5.03 4.04]	-1.27 [-5.47 2.93]
Cluster 2 Channel 50	Famous Faces vs. Scrambled	-4 [-13.82 5.82]	-4.11 [-15.62 7.40]	-4.04 [-13.31 5.23]
	Unfamiliar Faces vs. Scrambled	-2.16 [-9.20 4.87]	-2.17 [-9.83 5.48]	-2.32 [-8.96 4.31]
	Famous vs Unfamiliar Faces	-1.83 [-6.47 2.81]	-1.93 [-9.76 5.88]	-1.71 [-7.47 4.03]

Supplementary table 2. Pairwise differences in mean parameter estimates (arbitrary unit) measured at channel 50 and 6 at the maximum of the famous faces reponses.

		medianT	maxT	medianF	maxF	medianCluster	maxCluster	medianTFCE	maxTFCE
Face effect	OLS	4.44	157.64	2.09	74.19	72.57	22591.41	130.41	40992.1
	WLS	3.98	136.27	1.87	64.13	64.29	19453.52	85.72	35828.8
	IRLS	4.49	157.77	2.11	74.25	34.41	23300.19	130.88	54888.48
Repetition Effect	OLS	5.38	107.03	2.53	50.37	35.25	39116.91	244.38	82143.67
	WLS	4.46	109.14	2.1	51.36	33.76	33979.02	129.89	76244.1
	IRLS	5.32	110.86	2.5	52.17	37.31	39870.66	212.27	98429.06
Interaction Effect	OLS	5.45	126.31	1.12	26.01	23.79	387.94	27.64	483.46
	WLS	5.17	78.15	1.06	16.09	21.14	317.38	25.69	470.1
	IRLS	5.32	135.67	1.09	27.93	30.57	283.44	22.9	366.41

Supplementary table 3. Medians and maxima of the Hotelling T^2, F-values, Cluster-mass and TFCE scores for each effect of the ANOVA and methods used at the 1st level.

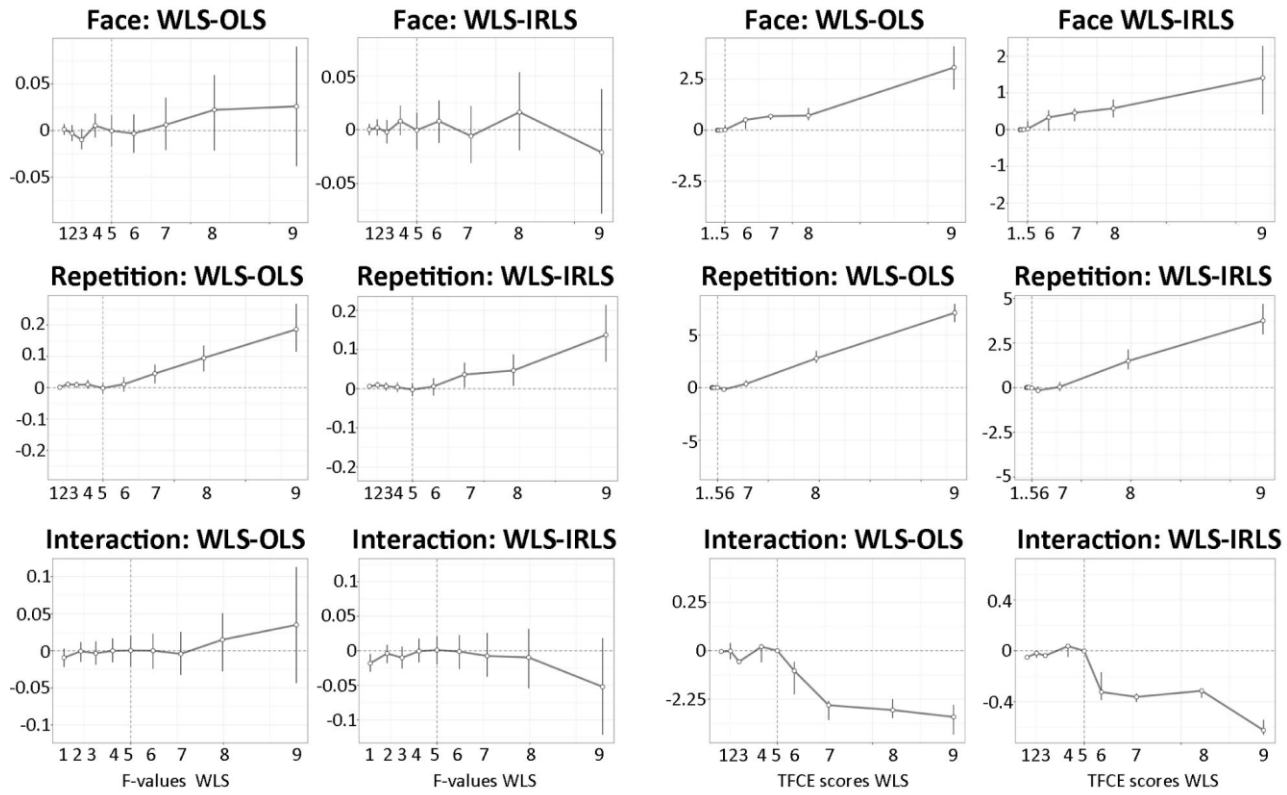

Figure 8. Shift function results comparing standardized F-value distributions for WLS to OLS and to IRLS for the face effect, repetition effect and their interaction.

Discussion

Simulation and data driven results indicate that the proposed WLS-PCP method is efficient at down weighting trials with dynamics differing from the bulk, leading to more accurate estimates. Results show that, for ERP, deriving weights based on the temporal profile provides a robust solution against white noise or uncontrolled oscillations. For biological (pink) noise and amplitude variations which do not alter the temporal profile, the PCP algorithm does not classify well outlier trials, leading to a decrease in detection performance compared with white, alpha or gamma noise. Rather than a defect, we see this as biologically relevant (see below). Importantly, even in those cases of failed detection, the overall correlations with the ground truth remained high (>=0.99). When analyzing real data, differences in amplitude variations were nevertheless captured by the PCP/WLS approach, with variations related to trials which were out of phase with the bulk of the data.

Group-level analyses of the face dataset replicated the main effect of face type (faces>scrambled) in a cluster from ~150ms to ~350ms but also revealed a late effect (>500ms), observed when using 1st level WLS and IRLS parameter estimates but absent when using OLS parameter estimates. Despite more data frames declared significant with WLS than OLS, effects sizes were smaller (and also smaller than IRLS). The shape of distributions when using WLS parameter

estrimates were however more right skewed than when using OLS or IRLS, leading clustering/tfce corrections to declare more data points as significant. Indeed under null, very similar distributions of maxima are observed leading to more power for the more skewed distributions. The interplay between 1st level regularization, 2nd level effect size, and multiple comparison procedures depends on many parameters and it is not entirely clear how statistical power is affected by their combination and requires deeper investigation via simulations. Empirically, we can nethertheless conclude that group results were statistically more powerful using robust approaches at the subject level than when using OLS.

Using the trial dynamics (temporal or spectral profile) to derive a single weight per trial makes sense, not just because the observed signal is autocorrelated, but also because it is biologically relevant. Let's consider first the signal plus noise model for ERP (Hillyard, 1985; Jervis et al., 1983; Shah, 2004). In this conceptualization, ERPs are time-locked additive events running on top of background activity. An outlier time frame for a given trial may occur if 1) the evoked amplitude deviates from the bulk, or 2) the background activity deviates from the rest of the background activity. In the former case, the additional signal may be conceived either as a single process (a chain of neural events at a particular location) or a mixture of processes (multiple, coordinated neural events). In both cases, the data generating process is thought to be evolving over time (auto-regressive) which speaks against flagging or weighting a strong deviation at a particular time frame only. What is likely, is that a minimum of consecutive time frames are seen as deviating, even though only one time frame is deemed an outlier. In the latter case (assuming no artefacts from recordings), a background deviation implies that for an extremely brief period of time, a large number of neurons synchronized for non-experimentally related reasons, and this event did not reoccur in other trials. Although we do not contend that such events cannot happen in general, this means that, in the context of ERP outlier detection, the background activity varies by an amount several folds bigger than the signal, which goes against theory and observations. Let's consider now the phase resetting model (Makeig, S. et al., 2002; Sayers et al., 1974). In this model, ERPs are emerging from the phase synchronization among trials, i.e., the occurrence of a stimulus reset the background activity. If a given trial deviates from the rest of other trials, this implies that it is out-of-phase. In this scenario, deriving different weights for different time frames (i.e. IRLS solution) means that the time course is seen as an alternation of 'normal' and outlying time frames, which has no meaningful physiological interpretation.

In conclusion, we propose a fast and straightforward weighting scheme for trials based on their temporal (or spectral) profiles. Results indicate that it captures well undesired noise leading to increased precision and possibly increased statistical power (more effect detected) at the group level.

Acknowledgements

Thank you to EEGLAB/LIMO MEEG users who engaged with the beta version, got stuck but persevered until we solved their issues.

References

Christensen, R. (2002). *Plane Answers to Complex Questions. The theory of Linear Models.* (3rd ed.). Springer.

Delorme, A., & Makeig, S. (2004). EEGLAB: An open source toolbox for analysis of single-trial EEG dynamics including independent component analysis. *Journal of Neuroscience Methods*, *134*(1), 9–21. https://doi.org/10.1016/j.jneumeth.2003.10.009

Filzmoser, P., Maronna, R., & Werner, M. (2008). Outlier identification in high dimensions. *Computational Statistics & Data Analysis*, *52*(3), 1694–1711.

Hillyard, S. A. (1985). Electrophysiology of human selective attention. *Trends in Neurosciences*, *8*, 400–405. https://doi.org/10.1016/0166-2236(85)90142-0

Hoaglin, D. C., & Welsch, R. E. (1978). The Hat Matrix in Regression and ANOVA. *The American Statistician*, *32*(1), 17–22. https://doi.org/10.2307/2683469

Jervis, B. W., Nichols, M. J., Johnson, T. E., Allen, E., & Hudson, N. R. (1983). A Fundamental Investigation of the Composition of Auditory Evoked Potentials. *Biomedical Engineering, IEEE Transactions On*, *BME-30*(1), 43–50. https://doi.org/10.1109/TBME.1983.325165

Kothe, C. A., & Makeig, S. (2013). BCILAB: A platform for brain-computer interface development. *Journal of Neural Engineering*, *10*(5), 056014. https://doi.org/10.1088/1741-2560/10/5/056014

Makeig, S., Westerfield, M., Jung, T-P., Enghoff, S., Townsend, J., Courchesne, E., & Sejnowski, T.J. (2002). Dynamic Brain Sources of Visual Evoked Responses. *Science*, *295*(5555), 690–694.

Maris, E. & Oostenveld, R. (2007). Nonparametric statistical testing of EEG- and MEG-data. *Journal of Neuroscience Methods*, *164*(1), 177–190.

Onton, J., Westerfield, M., Townsend, J., & Makeig, S. (2006). Imaging human EEG dynamics using independent component analysis. *Neuroscience & Biobehavioral Reviews*, *30*(6), 808–822. https://doi.org/10.1016/j.neubiorev.2006.06.007

Pernet, C.R., Latinus, M., Nichols, T. E., & Rousselet, G. A. (2015). Cluster-based computational methods for mass univariate analyses of event-related brain potentials/fields: A simulation study. *Journal of Neuroscience Methods*, *250*, 85–93. https://doi.org/10.1016/j.jneumeth.2014.08.003

Pernet, C.R., Appelhoff, S., Gorgolewski, K. J., Flandin, G., Phillips, C., Delorme, A., & Oostenveld, R. (2019). EEG-BIDS, an extension to the brain imaging data structure for electroencephalography. *Scientific Data*, *6*(1), 103. https://doi.org/10.1038/s41597-019-0104-8

Pernet, C.R., Chauveau, N., Gaspar, C., & Rousselet, G. A. (2011). LIMO EEG: A Toolbox for Hierarchical LInear MOdeling of ElectroEncephaloGraphic Data. *Computational Intelligence and Neuroscience*, *2011*, 1–11. https://doi.org/10.1155/2011/831409

Pernet, C.R., Martinez-Cancino, R., Truong, D., Makeig, S., & Delorme, A. (2021). From BIDS-Formatted EEG Data to Sensor-Space Group Results: A Fully Reproducible Workflow With EEGLAB and LIMO EEG. *Frontiers in Neuroscience*, *14*, 610388. https://doi.org/10.3389/fnins.2020.610388

Pion-Tonachini, L., Kreutz-Delgado, K., & Makeig, S. (2019). The ICLabel dataset of electroencephalographic (EEG) independent component (IC) features. *Data in Brief*, *25*,

104101. https://doi.org/10.1016/j.dib.2019.104101

Sayers, B. MCA., Beagley, H. A., & Henshall, W. R. (1974). The Mechanism of Auditory Evoked EEG Responses. *Nature*, *247*(5441), 481–483. https://doi.org/10.1038/247481a0

Shah, A. S. (2004). Neural Dynamics and the Fundamental Mechanisms of Event-related Brain Potentials. *Cerebral Cortex*, *14*(5), 476–483. https://doi.org/10.1093/cercor/bhh009

Yeung, N., Bogacz, R., Holroyd, C., Nieuwenhuis, S., & Cohen, J. (2018). *Simulated EEG data generator* [Matlab]. https://data.mrc.ox.ac.uk/data-set/simulated-eeg-data-generator